



ELSEVIER

Contents lists available at [SciVerse ScienceDirect](http://www.sciencedirect.com)

Journal of Theoretical Biology

journal homepage: [www.elsevier.com/locate/yjtbi](http://www.elsevier.com/locate/yjtbi)

## Neutrophil dynamics after chemotherapy and G-CSF: The role of pharmacokinetics in shaping the response

Grace Brooks<sup>a</sup>, Gabriel Provencher<sup>b</sup>, Jinzhi Lei<sup>c,\*</sup>, Michael C. Mackey<sup>d</sup>

<sup>a</sup> Departments of Physiology and Physics, Centre for Applied Mathematics in Bioscience and Medicine, McGill University, Montreal, QC, Canada H4X 2C1

<sup>b</sup> Departments of Mathematics and Physics, Centre for Applied Mathematics in Bioscience and Medicine, McGill University, Montreal, QC, Canada H4X 2C1

<sup>c</sup> Zhou Pei-Yuan Center for Applied Mathematics, Tsinghua University, Beijing 100084, China

<sup>d</sup> Departments of Physiology, Physics, and Mathematics, Centre for Applied Mathematics in Bioscience and Medicine, McGill University, Montreal, QC, Canada H4X 2C1

### ARTICLE INFO

#### Article history:

Received 19 January 2012

Received in revised form

21 July 2012

Accepted 23 August 2012

Available online 7 September 2012

#### Keywords:

Neutropenia

Mathematical model

Recovery rate

Resonance

Cancer

### ABSTRACT

Chemotherapy has profound effects on the hematopoietic system, most notably leading to neutropenia. Granulocyte colony stimulating factor (G-CSF) is often used to deal with this neutropenia, but the response is highly variable. In this paper we examine the role of pharmacokinetics and delivery protocols in shaping the neutrophil responses to chemotherapy and G-CSF. Neutrophil responses to different protocols of chemotherapy administration with varying dosages, infusion times, and schedules are studied through a mathematical model. We find that a single dose of chemotherapy produces a damped oscillation in neutrophil levels, and short-term applications of chemotherapy can induce permanent oscillations in neutrophil level if there is a bistability in the system. In addition, we confirm previous findings [Zhuge et al., *J. Theor. Biol.*, 293(2012), 111–120] that when periodic chemotherapy is given, there is a significant period of delivery that induces resonance in the system and exacerbates the corresponding neutropenia. The width of this resonant period peak increases with the recovery rate after a single chemotherapy, which is given by the real part of the dominant eigenvalue pair at the steady state, and both are determined by a single cooperativity coefficient in the feedback function for the neutrophils. Our numerical studies show that the neutropenia caused by chemotherapy can be overcome if G-CSF is given early after chemotherapy but can actually be worsened if G-CSF is given later, consistent with results reported in Zhuge et al. (2012). The nadir in neutrophil level is found to be more sensitive to the dosage of chemotherapy than that of the G-CSF. Furthermore, dependence of our results with changes in key pharmacokinetic parameters as well as initial functions are studied. Thus, this study illuminates the potential for destructive resonance leading to neutropenia in response to periodic chemotherapy, and explores and explains why the timing of G-CSF is so crucial for successful reversal of chemotherapy induced neutropenia.

© 2012 Elsevier Ltd. All rights reserved.

### 1. Introduction

The chemotherapeutic treatment of malignant tumors is widespread but lacks a strong theoretical understanding of its efficacy and side effects. Chemotherapy is frequently accompanied by hematopoietic side effects due to the myelosuppressive character of the drugs used. These side effects commonly include neutropenia (accompanied by fever and possible infection) and, less frequently, thrombocytopenia and/or anemia (Rahman et al., 1997; Vainstein et al., 2005a). Administration of recombinant hematopoietic cytokines following chemotherapy is frequently used in an effort to circumvent these side effects. Thus, granulocyte colony stimulating factor (G-CSF) is now a

standard post-chemotherapy treatment for neutropenia (Crawford et al., 2003; Foley and Mackey, 2009).

The interval (period) between repeated administration of chemotherapy is known to have effects on the hematopoietic response (Thatcher et al., 2000; Tjan-Heijnen et al., 2002), and the neutrophil response to G-CSF is highly variable and depends on the timing and protocol of the drug's administration (Morstyn et al., 1989; Meisenberg et al., 1992; Butler et al., 1992; Fukuda et al., 1993; Koumakis et al., 1999; Vainstein et al., 2005a). Over the past decades, much effort has been expended trying to quantify the hematopoietic response to chemotherapy and G-CSF, both clinically and through mathematical modeling, and in the Discussion we survey some of the modeling efforts in this direction.

Zhuce et al. (2012) used a mathematical model of the combined dynamics of the hematopoietic stem cells and the differentiated neutrophil progeny to examine the effects of repeated

\* Corresponding author. Tel.: +86 10 62795156; fax: +86 10 62797075.

E-mail addresses: [jzlei@mail.tsinghua.edu.cn](mailto:jzlei@mail.tsinghua.edu.cn) (J. Lei), [michael.mackey@mcgill.ca](mailto:michael.mackey@mcgill.ca) (M.C. Mackey).

and periodic chemotherapy in generating neutropenia, and the corresponding response to G-CSF intended to counteract the neutropenia. They found that if chemotherapy is given alone every  $T$  days, there is a significant period  $T_R$  of administration (with  $T_R$  twice the average neutrophil lifespan from commitment to death) that can induce resonance and neutropenia in the system. This finding suggests that myelosuppressive protocols should avoid this period to minimize hematopoietic damage. A similar resonance in the face of periodic chemotherapy was also noted in a modeling study of acute myelogenous leukemia (Andersen and Mackey, 2001). However, the Zhuge et al. (2012) study did not consider the pharmacokinetics of either the chemotherapy or the G-CSF and therefore it is not clear whether these results would still hold in a more realistic model and, more importantly, whether they are valid clinically.

In this paper we expand a dynamic model for the stem cells and neutrophils to include the pharmacokinetics of chemotherapy and G-CSF, and use this to study neutrophil responses to different protocols of chemotherapy administration including varying dosages, infusion times and schedules, and re-examine the dependence of the neutrophil response on the period of simulated chemotherapy and secondary G-CSF administration as in Zhuge et al. (2012). Thus this paper extends the previous studies in Zhuge et al. (2012), aimed at understanding how different protocols can shape the responses. We further amplify the understanding of how the previous results depend on changes in key parameters and the history functions prior to the administration of chemotherapy, since both may vary between patients.

## 2. The model

### 2.1. The model equations

Fig. 1 illustrates the two compartmental model of neutrophil production presented in Zhuge et al. (2012) that we extend in this paper. We summarize the model description below and refer to Zhuge et al. (2012) for details.

This model includes the dynamics of the hematopoietic stem cells (HSC) in the resting phase as well as circulating neutrophils. HSCs can either remain in the resting phase (population  $Q$ , cells/kg), exit into the proliferative phase at a rate  $\beta$  (days<sup>-1</sup>), or differentiate into the committed neutrophil compartment at a rate  $\kappa_N$  (days<sup>-1</sup>), or into the megakaryocyte and erythrocyte lines at a combined rate  $\kappa_\delta$  (days<sup>-1</sup>). Cells in the HSC proliferative phase are assumed to undergo apoptosis at a rate  $\gamma_S$  (days<sup>-1</sup>) and the duration of the proliferative phase is taken to be  $\tau_S$  (days). Cells in the neutrophil pathway are amplified by successive divisions over a time period of duration of  $\tau_{NP}$  (days) through proliferation at a rate  $\eta_{NP}$  (days<sup>-1</sup>). Following the cessation of proliferation they enter a purely maturation (no proliferation) compartment for a period of time  $\tau_{NM}$  (days) while dying randomly at a rate  $\gamma_0$  (days<sup>-1</sup>) before they enter the circulation. The circulating neutrophils (population  $N$ , cells/kg) die randomly at a rate  $\gamma_N$  (days<sup>-1</sup>) so their average lifespan is  $\gamma_N^{-1}$ . The rate of differentiation of HSCs to neutrophils is controlled by the

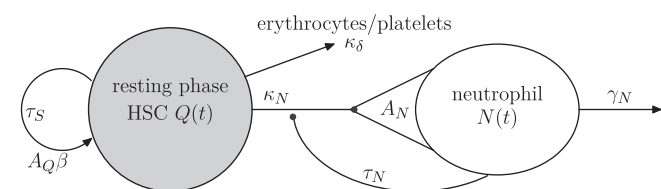


Fig. 1. A cartoon representation of the two compartmental model of neutrophil production investigated here. Refer to the text and Zhuge et al. (2012) for details.

circulating neutrophil population through the differentiation rate  $\kappa_N(N)$ , and the HSCs proliferation is controlled by the resting HSC population through the proliferation rate  $\beta(Q)$ .

The mathematical formulation for this abstraction of the neutrophil production system is described by an age structured model, and the integration of this age structured model in conjunction with the appropriate boundary conditions yields a system of two delay differential equations (c.f. Bernard et al., 2003; Foley and Mackey, 2009; Lei and Mackey, 2011; Zhuge et al., 2012). Each of these equations takes into account the balance between the net production and loss rates of HSCs and circulating neutrophils. It is the resulting delay differential equation model we are studying here. We always use the convention that a variable delayed by a time  $\tau$ , e.g.  $x(t-\tau)$ , is denoted by  $x_\tau$ . With this convention, the equations describing the dynamics of this model are given by

$$dQ/dt = -(\beta(Q) + \kappa_N(N) + \kappa_\delta)Q + A_Q(t)\beta(Q_{\tau_S})Q_{\tau_S} \tag{1}$$

$$dN/dt = -\gamma_N N + A_N(t)\kappa_N(N_{\tau_N})Q_{\tau_N}, \tag{2}$$

where

$$\kappa_N(N) = f_0 \theta_N^{s_1} / (\theta_N^{s_1} + N^{s_1}),$$

$$\beta(Q) = k_0 \theta_S^{s_2} / (\theta_S^{s_2} + Q^{s_2}),$$

$$A_Q(t) = 2 \exp \left[ - \int_0^{\tau_S} \gamma_S(t - \tau_S + s) ds \right]$$

$$A_N(t) = \exp \left[ \int_0^{\tau_{NP}} \eta_{NP}(t - \tau_N(t) + s) ds \right.$$

$$\left. - \int_{\tau_{NP}}^{\tau_N(t)} \gamma_0(t - \tau_N(t) + s) ds \right].$$

$$\tau_N(t) = \tau_{NP} + \tau_{NM}(t).$$

For hematologically normal individuals, the rates  $\gamma_S, \eta_{NP}$  and  $\gamma_0$  are constants, and therefore

$$A_Q = 2e^{-\gamma_S \tau_S}, \quad A_N = e^{\eta_{NP} \tau_{NP} - \gamma_0 \tau_{NM}}. \tag{3}$$

Notice that in the above equations, the rates  $\gamma_S, \eta_{NP}, \gamma_0$ , and the neutrophil maturation time  $\tau_{NM}$  are time dependent because of effects of chemotherapy and G-CSF which are described below.

We have estimated parameters for hematologically normal individuals, which are given in Table 1 in Appendix B. (A critical change in the parameters, compared to Zhuge et al. (2012), is in the value of  $s_1$  which we find essential for the recovery rate after a single application of chemotherapy and the resonant peak width in the case of periodic application of chemotherapy, detailed below).

### 2.2. Simulating chemotherapy

There are many different chemotherapeutic drugs currently in use, and their modes of administration are either by direct intravenous infusion or by oral administration. After the drug enters the body, it is usually modeled as being distributed amongst several compartments, which may or may not have physiological correlates. This study intends to investigate neutrophil dynamics after chemotherapy in a general sense, and we do not study the detailed route of administration, nor do we consider the pharmacokinetics in different tissue compartments. Thus, we consider a single compartment model with a moderately rapid clearance that is characteristic of a number of common chemotherapeutic agents (Minkin et al., 2008; Fogli et al., 2001; Henningsson et al., 2001; Mou et al., 1997; Morikawa et al., 1997; Peng et al., 2004; Vainstein et al., 2005a). Despite its simplicity, our model captures the essential dynamics, and using a more complex multi-compartment model does not affect the results we have obtained (data not included). Such multi-compartmental models are usually developed for specific drugs (for example, see Sparreboom

**Table 1**

Estimated equilibrium values for normal subjects.

Sources: 1=Bernard et al. (2003), 2=Mackey (2001), 3=Bernard et al. (2003a), 4=Hearn et al. (1998), 5=Haurie et al. (2000), 6=Colijn and Mackey (2005b), 7=Henningson et al. (2001), 8=Israels and Israels (2002), 9=Foley and Mackey (2009), 10=Novak and Nečas (1994), 11=Dancey et al. (1976), 12=Calculated.

Parameters name	Value used	Unit	Sources
<i>Stem cell compartment</i>			
$Q_*$	1.12	$10^6$ cells/kg	1
$\gamma_S$	0.1043	days <sup>-1</sup>	1, 2
$\gamma_S^{\min}$	0.03	days <sup>-1</sup>	1
$\gamma_S^{\max}$	0.40	days <sup>-1</sup>	9
$\tau_S$	2.83	days	1, 2
$k_0$	8.0	days <sup>-1</sup>	1, 3
$\theta_2$	0.0826	$10^6$ cells/kg	2, 12
$s_2$	2	(none)	1
<i>Neutrophil compartment</i>			
$N_*$	5.59	$10^8$ cells/kg	11
$\gamma_N$	2.4	days <sup>-1</sup>	1, 5
$b_n$	0.05	mg/ml	9
$\tau_N$	9.7	days	4
$\tau_{NP}^{\max}$	3.8	days	4
$\tau_{NP}$	5.9	days	12, 13
$b_v$	0.001	$\mu$ g/ml	9
$V_{\max}$	3.8		
$\eta_{NP}$	2.1995	days <sup>-1</sup>	12
$\eta_{NP}^{\min}$	0.4	days <sup>-1</sup>	12
$\eta_{NP}^{\max}$	2.5444	days	
$A_N$	1549.58	$10^2$	12
$\gamma_0$	0.27	days <sup>-1</sup>	
$\gamma_0^{\min}$	0.12	days <sup>-1</sup>	
$f_0$	0.154605	days <sup>-1</sup>	1
$\theta_1$	0.0154848	$10^8$ cells/kg	12
$s_1$	0.5	(none)	12
<i>Other cell compartments</i>			
$\kappa_\delta$	0.0134	days <sup>-1</sup>	6
<i>G-CSF compartment</i>			
$X_*$	0.1	$\mu$ g/kg	10
$G_*$	0	$\mu$ g/ml	10
$V_B$	76	ml/kg	10, 11
$G_{\text{prod}}$	0	$\mu$ g/(ml $\times$ day)	9
$k_T$	1.68	days <sup>-1</sup>	10, 11
$k_B$	6.4	days <sup>-1</sup>	10
$\sigma$	0.72	kg/day	10, 8
$\gamma_G$	4.36	days <sup>-1</sup>	9
$k$	10	( $\mu$ g/ml) <sup>2</sup>	9
<i>Chemotherapy</i>			
$\delta$	100	days <sup>-1</sup>	7
$\phi$	32.07	days <sup>-1</sup>	7
$h_S$	0.0702	kg/(mg $\times$ day)	12
$h_{NP}$	0.4275	kg/(mg $\times$ day)	12

et al., 2003; Gianni et al., 2011; Henningson et al., 2001 for models of Paclitaxel administration).

We denote the active plasma chemotherapy drug concentration by  $C(t)$  that consists of an exponentially increasing portion until a maximum value at the end of administration and then followed by a falling phase back to zero. This assumption is in agreement with experimental observations (Gianni et al., 2011; Fetterly et al., 2008; Vainstein et al., 2005a). After a single administration of chemotherapy these rising and falling phases can be described by

$$C(t) = (I_0/\phi) \begin{cases} (1 - e^{-\delta t}), & 0 \leq t \leq \Delta_c \\ (1 - e^{-\delta \Delta_c})e^{-\delta(t - \Delta_c)}, & \Delta_c < t. \end{cases} \quad (4)$$

Here,  $\Delta_c$  (days) is the duration of the rising phase (infusion time) of the chemotherapy,  $I_0$  (mg/(kg  $\times$  day)) measures the injection

rate of drug into the plasma,  $\phi$  (days<sup>-1</sup>) is the clearance rate of drug from the body, and  $\delta$  (days<sup>-1</sup>) is the effective rate constant of removal of the chemotherapeutic drug. The total amount of chemotherapy drug administered in the plasma (dosage  $D$ , mg/kg) is therefore given by

$$D = I_0 \Delta_c. \quad (5)$$

Thus the injection rate is expressed through the infusion time  $\Delta_c$  and dosage  $D$  as

$$I_0 = D/\Delta_c. \quad (6)$$

The decay time of a drug varies with the chemotherapeutic agent being used. Here  $\delta = 100$  days<sup>-1</sup> is used corresponding to the drug Taxol (Henningson et al., 2001). We also choose dosage units to mimic Taxol, such that a standard dosage of 135 mg/kg is capable of causing severe neutropenia with periodic administration every 3 weeks.

Since we are interested in determining the effects of multiple doses of chemotherapy delivered with period  $T$ , we extend this formulation in the following way. In each time period  $[jT, (j+1)T)$ , a single dose of chemotherapy is administered in the interval  $jT \leq t \leq jT + \Delta_c$ , and we have approximately

$$C(t) = \begin{cases} I_0(1 - e^{-\delta(t - jT)}), & \text{if } jT \leq t \leq jT + \Delta_c \\ I_0(1 - e^{-\delta \Delta_c})e^{-\delta(t - jT - \Delta_c)}, & \text{if } (jT + \Delta_c) \leq t \leq (j+1)T \end{cases} \quad (7)$$

In the current model, let  $\gamma_S^{\text{chemo}}(t)$  be the stem cell apoptosis rate which is dependent on the concentration of chemotherapy. For relatively short durations  $\Delta_c$  of chemotherapy infusion, there is an approximately linear relationship between  $C(t)$  and the apoptosis rate (Karl et al., 2011), so we assume

$$\gamma_S^{\text{chemo}}(t) = \gamma_S(0) + h_S C(t) \quad (8)$$

with  $\gamma_S(0)$  the default apoptosis rate before chemotherapy, and  $h_S$  is a constant to be determined.

Similarly, let  $\eta_{NP}^{\text{chemo}}(t)$  be the neutrophil amplification rate which is also dependent on the chemotherapy. Since

$\eta_{NP}$  = proliferation rate – apoptosis rate

during chemotherapy we write

$$\eta_{NP}^{\text{chemo}}(t) = \eta_{NP}(0) - h_{NP} C(t), \quad (9)$$

where  $\eta_{NP}(0)$  is the amplification rate in the absence of chemotherapy, and  $h_{NP}$  is also a rate constant.

### 2.3. Simulating G-CSF administration

The model for G-CSF pharmacokinetics studied here is adapted from Colijn et al. (2007) (also see Foley and Mackey, 2009) that consists of two compartments consisting of tissue and the circulation system (Fig. 2).

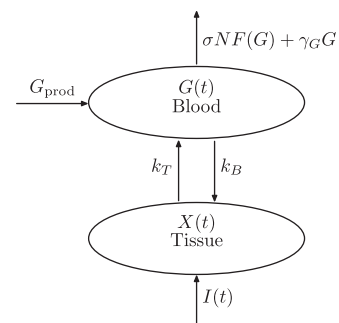


**Fig. 2.** A two-compartment model for subcutaneous administration of G-CSF.  $I(t)$  is a step function representing injection of exogenous G-CSF into the tissue. Redrawn from Foley and Mackey (2009).

Let  $X(t)$  ( $\mu\text{g}/\text{kg}$ ) denotes the tissue level of G-CSF,  $G(t)$  ( $\mu\text{g}/\text{ml}$ ) the circulating G-CSF concentration, and  $I(t)$  a step function representing the injection of exogenous G-CSF into the tissues. We can write the dynamic equation for the G-CSF administration in the form (Foley and Mackey, 2009)

$$dX/dt = I(t) + k_T V_B G - k_B X \quad (10)$$

$$dG/dt = G_{\text{prod}} + k_B X/V_B - k_T G - (\gamma_G G + \sigma NF(G)). \quad (11)$$

Here  $k_T$  and  $k_B$  are rate constants for the exchange between the blood and tissue compartments, and  $V_B$  is the volume of the blood compartment in order to make the units of  $G$  and  $X$  agree in both equations. In the second equation,  $G_{\text{prod}}$  is the fixed G-CSF production rate, and the clearance is given by two parts: the degradation of G-CSF by the kidneys at a rate  $\gamma_G$ , and the removal of G-CSF from the circulation through a saturable clearance  $\sigma NF(G)$  where (see Appendix A)

$$F(G) = \frac{G^2}{k_G + G^2}, \quad (12)$$

In modeling, a single injection starting from  $t = t_{\text{on}}$  and with duration  $s$  is mimicked by a step function

$$I(t) = (a/s)[H(t-t_{\text{on}})(1-H(t-t_{\text{on}}+s))], \quad (13)$$

where  $a$  measures the dosage given in a bolus injection, and  $H(t)$  is the Heaviside function defined as

$$H(t) = \begin{cases} 0, & t < 0 \\ 1, & t \geq 0 \end{cases} \quad (14)$$

The parameters  $a$  and  $s$  differ with different forms of G-CSF, *i.e.* filgrastim versus pegfilgrastim. Here, we study the effect of filgrastim, and from Foley and Mackey (2009) take  $a=5$  or  $10 \mu\text{g}/\text{kg}$  and  $s = 0.0083$  day in our simulations.

G-CSF is known to perturb the hematopoietic dynamics by decreasing the apoptosis rate of the HSC (Merchant et al., 2011), reducing the apoptosis rate of the committed neutrophils (Leavey et al., 1998), and decreasing the neutrophil precursor maturation time (Price et al., 1996). Using  $G(t)$  in the current model, the effects of G-CSF administration are modeled by

$$\gamma_S(t) = \gamma_S^{\text{min}} + (\gamma_S^{\text{chemo}}(t) - \gamma_S^{\text{min}}) \frac{b_S}{G(t) + b_S}, \quad (15)$$

$$\gamma_0(t) = \gamma_0^{\text{min}} + (\gamma_0 - \gamma_0^{\text{min}}) \frac{b_0}{G(t) + b_0}, \quad (16)$$

$$\eta_{NP}(t) = \eta_{NP}^{\text{chemo}}(t) + (\eta_{NP}^{\text{max}} - \eta_{NP}^{\text{chemo}}(t)) \frac{G(t)}{G(t) + c_n}, \quad (17)$$

and

$$\tau_{NM}(t) = \tau_{NM}^{\text{max}} / V_n(t), \quad V_n(t) = 1 + (V_{\text{max}} - 1) \frac{G(t)}{G(t) + b_v}. \quad (18)$$

From the (8), (9), (15), (17), the rates  $\gamma_S$  and  $\eta_{NP}$  are modeled by the following: when  $jT < t \leq (j+1)T$ , let

$$\gamma_S(t) = \gamma_S^{\text{min}} + (\gamma_S^{\text{chemo}}(t) - \gamma_S^{\text{min}}) \frac{b_S}{G(t) + b_S} \\ \gamma_S^{\text{chemo}}(t) = \gamma_S(jT) + h_S C(t), \quad (19)$$

and

$$\eta_{NP}(t) = \eta_{NP}^{\text{chemo}}(t) + (\eta_{NP}^{\text{max}} - \eta_{NP}^{\text{chemo}}(t)) \frac{G(t)}{G(t) + c_n}, \\ \eta_{NP}^{\text{chemo}}(t) = \eta_{NP}(jT) - h_{NP} C(t). \quad (20)$$

Here  $C(t)$  and  $G(t)$  are given by (7) and (10)–(11), respectively.

#### 2.4. Numerical techniques

We numerically solve the model equations using the Euler method for the delay differential equations with the parameters of Table 1, and an integration step size  $\Delta t = 0.001$  day. In the integration, if not specified explicitly, we start from a constant initial function  $(Q(t), N(t)) = (Q_*, N_*)$  for  $t < 0$ , consistent with the steady state of a normal individual. The simulation code is written in C++, and is available upon request.

### 3. Results

#### 3.1. Effects of a single application of chemotherapy

First we quantify the effect of a single application of chemotherapy with varying dosage  $D$  (from 0 to 295 mg/kg) and the infusion time  $\Delta_c$  (from 1 to 24 h) (Fig. 3). Simulations show that a single chemotherapy treatment induces a significant reduction in the number of stem cells and neutrophils, followed by a recovery stage during which the neutrophil count displays a damped oscillatory return to the normal level steady state with an oscillation period of 20 days and a recovery rate of  $0.074 \text{ days}^{-1}$ , *i.e.*, the circulating neutrophils regain their normal level after two cycles of oscillation (Fig. 3a). Changes in the infusion time have only a small effect on the neutrophil response. An infusion time of 24 h produces

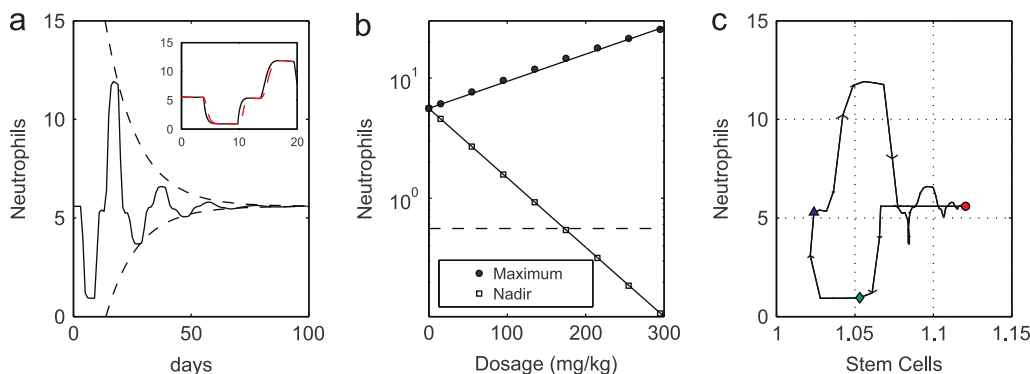


**Fig. 3.** Numerical simulation of neutrophil response to a single dose of chemotherapy. (a) Neutrophil time course after a single dose of chemotherapy. Here the dosage  $D = 135 \text{ mg}/\text{kg}$  and the infusion time  $\Delta_c = 1 \text{ h}$  (starting from  $t=0$ ). Dashed lines show fitting of the maximum and nadir levels with recovery rate  $0.074 \text{ days}^{-1}$ . Inset shows simulations with  $\Delta_c = 1 \text{ h}$  (black solid line) and  $\Delta_c = 24 \text{ h}$  (dashed line), respectively. (b) Dependence of neutrophil maximum and nadir levels after a single dose of chemotherapy. Markers are obtained from simulations, while solid lines are the fits with Eqs. (21). (c) Phase plane plot of neutrophil vs. stem cell counts ( $D = 135 \text{ mg}/\text{kg}$ ,  $\Delta_c = 1 \text{ h}$ ). Arrows show the direction of increasing time. Three specific time points are marked by the red circle ( $t=0$ ), green diamond ( $t=4$  days) and blue triangle ( $t=9$  days), respectively (refer to the text for further detail). Neutrophil levels are in units of  $10^8$  cells/kg, stem cell level are in units of  $10^6$  cells/kg. (For interpretation of the references to color in this figure caption, the reader is referred to the web version of this article.)



a slight delay in the neutrophil response, but no effect on the maximum and nadir neutrophil levels or oscillation period, compared to the infusion time of 1 h (and with the same dosage) (Fig. 3a inset). Both maximum and nadir levels depend on the dosages exponentially as (Fig. 3b)

$$\begin{aligned} \text{Maximum} &= 5.59e^{0.0052D} \\ \text{Nadir} &= 5.59e^{-0.0133D} \end{aligned} \quad (21)$$

We also note that the stem cell count decreases immediately after chemotherapy administration, while neutrophils respond with a lag time of 4 days and drop to their lowest level at about 9 days after the chemotherapy administration (Fig. 3c). The postponed response of the neutrophils is due to the delay in neutrophil precursor maturation, and is in agreement with clinical observations, where the time of the nadir in the circulating neutrophils ranges from 7 to 14 days (Green et al., 2003).

In simulations, the neutrophil dynamics in the recovery stage are independent of the dosage and infusion time (data not shown). Theoretically, the recovery rate is determined from the linearization of the model equations (1) and (2) near the steady state. The steady state of a normal individual is assumed to be stable, therefore all eigenvalues of the linearized equation should have negative real parts, each of which gives a corresponding damping rate after a small perturbation that is defined by the absolute value of the real part. The recovery rate after a single application of chemotherapy is then given by the minimum of all these rates. In Appendix C, we analyze the dependence of the recovery rate based on a single equation model of the neutrophil dynamics. We show that the recovery rate decreases with  $\tau_N$  and the coefficient  $s_1$  in the feedback function  $\kappa_N(N)$  approximately as (refer to Fig. 11)

$$\text{Recovery rate} \approx -\tau_N^{-1} \ln s_1. \quad (22)$$

The coefficient  $s_1$  is a phenomenological parameter, and there is no experimental data available to aid in estimating its value. Our results thus provide a way to estimate this coefficient through a single perturbation in neutrophil counts by chemotherapy and then subsequent measurement of the recovery dynamics.

In these simulations, we have assumed the initial function to be constant at the normal steady state ( $Q_*, N_*$ ). However, in many clinical situations, the hematopoietic dynamics of a patient before chemotherapy administration may deviate from the normal state or even fluctuating due to previous perturbations. Here we examine how the above results depend on the initial functions by examining the neutrophil response with initial functions of either oscillatory or abnormally high neutrophil levels with stochastic fluctuations (Fig. 4). The simulations show that changes in the initial function may alter the maximum and nadir neutrophil level, but have no effect on either the oscillation period (same as the resonance period discussed below) or the recovery rate after a single application of chemotherapy.

### 3.2. Effect of short chemotherapy protocols in developing a stationary state

Short term chemotherapy of a few months is suggested in some clinical situations. For example, adjuvant chemotherapy (after surgery) tends to last between 5 and 12 months (Levine and Whelan, 2006). An interesting question is whether short-term chemotherapy can induce permanent oscillations in the neutrophil dynamics. Here, we study this issue numerically and show that the answer is parameter dependent.

First, we simulate the neutrophil response with the parameters as in Table 1, and fix the period of chemotherapy administration at  $T=21$  days, but stop the chemotherapy after a few applications (ranging from 1 to 6 applications). We also

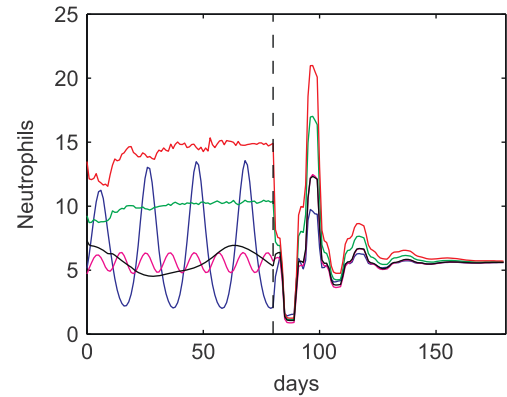


**Fig. 4.** Numerical simulations of neutrophil dependence after a single application of chemotherapy, with different initial functions. Dashed line shows the day of chemotherapy administration. In simulations,  $D = 135$  mg/kg and  $A_c = 1$  h. Initial functions are assigned by replacing the coefficients  $A_Q(t)$  and  $A_N(t)$  by  $A_Q(t)(1+r_1(t))$  and  $A_N(t)(1+r_2(t))$  before chemotherapy administration, with  $r_i(t) = 0.5 \sin(0.3t)$  (blue),  $0.2 \sin(0.6t)$  (magenta), or  $0.3 \sin(0.1t)$  (black) for periodic initial functions, and independent random numbers  $r_i$  uniformly distributed on the intervals  $[0,2]$  (red) or  $[0,1]$  (green) for abnormally high neutrophil levels with stochastic fluctuations. Neutrophil levels are in units of  $10^8$  cells/kg. (For interpretation of the references to color in this figure caption, the reader is referred to the web version of this article.)

varied the dosage  $D$  over the range from 95 to 175 mg/kg. Simulations show that in all cases neutrophil levels oscillate during the chemotherapy administration, and then recover to their normal steady state at a rate of  $0.074 \text{ days}^{-1}$  after the chemotherapy administration is stopped. This is similar to the case of a single application (see for example Fig. 5a). Thus, using the parameters as in Table 1, a finite application of chemotherapy would not induce sustained oscillations in neutrophil dynamics.

Next, we adjust the parameters so that the model has multi-stability with a co-existence of stable oscillation and steady state solutions. The existence of such multi-stability of the hematopoietic dynamics model has been studied in Bernard et al. (2003) and in Lei and Mackey (2011), and Foley et al. (2006) (Fig. 9) contains experimental evidence for this multistability. We take  $\kappa_\delta = 0.145$  with the other parameters as in Table 1. The simulations are shown in Fig. 5. From the simulation, if only one chemotherapy is applied, the neutrophil dynamics recover to the normal level after the chemotherapy is stopped. However, if three or more chemotherapy cycles are applied, the chemotherapy induces permanent oscillatory dynamics even after cessation of the chemotherapy. Thus, when  $\kappa_\delta = 0.145$ , it is possible to induce permanent oscillations in neutrophil dynamics after a few rounds of chemotherapy. We note that  $\kappa_\delta$  denotes the total differentiation rate of HSC into the megakaryocyte and erythrocyte lines, which is subject to feedback regulation by the erythrocyte and platelet populations (Colijn and Mackey, 2005a). A decrease in red blood cell and/or platelet level may give rise to an increase in the differentiation rate  $\kappa_\delta$ . In this case, our simulations suggest that it may be possible to induce cyclical neutropenia with a finite number of chemotherapy treatments. However, this result remains to be verified through a more comprehensive model including both erythrocyte and platelet cell lines and will be a subject for future investigation.

### 3.3. Effects of periodic application of chemotherapy

Zhugue et al. (2012) found that if chemotherapy is given periodically, there is a significant period  $T$  of administration that can induce resonance in the system and a corresponding neutropenia. There have been at least two reports in the clinical literature of sustained neutrophil oscillations in patients receiving

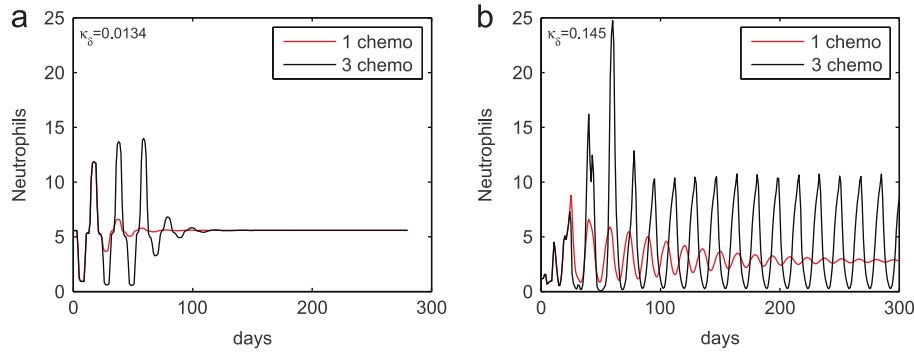


**Fig. 5.** Neutrophil dynamics with either 1 or 3 (with an interval of 21 days) chemotherapy administrations, with different values of the differentiation rate  $\kappa_0$ : (a)  $\kappa_0 = 0.0134$  and (b)  $\kappa_0 = 0.145$ , and other parameters as in Table 1. The dosage  $D = 135$  mg/kg, infusion time  $\Delta_c = 1$  h. Neutrophil levels are in units of  $10^8$  cells/kg.

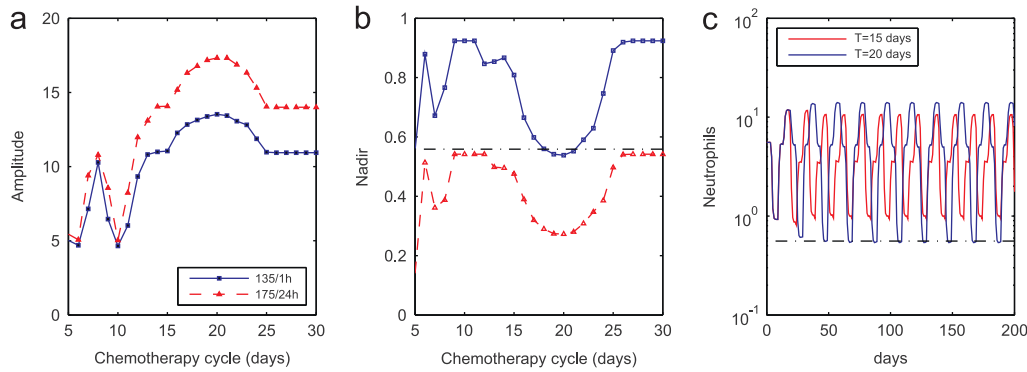


**Fig. 6.** Numerical simulation results of periodic administration of chemotherapy with varying period  $T$ , dosage  $D$  and infusion time  $\Delta_c$ . (a) The amplitude in neutrophil response is shown as a function of the period of  $T$  of chemotherapy, with  $(D, \Delta_c) = (135$  mg/kg, 1 h) (blue squares connected with a solid line) and  $(175$  mg/kg, 24 h) (red triangle connected with a dashed line), respectively. (b) The nadir as a function of  $T$ , with parameters and markers same as in (a). The horizontal black dashed-dot line indicates the level for severe neutropenia ( $0.56 \times 10^8$  cells/kg). (c) Simulated neutrophil levels in response to chemotherapy with a period of either  $T = 15$  days or  $T = 20$  days, with  $D = 135$  mg/kg and  $\Delta_c = 1$  h. Neutrophil levels are in units of  $10^8$  cells/kg, the dashed-dot horizontal line again indicates the level for severe neutropenia. (For interpretation of the references to color in this figure caption, the reader is referred to the web version of this article.)

long term chemotherapy (David et al., 1973; Kennedy, 1970). To study the neutrophil response to periodic chemotherapy, we vary  $T$  from 5 to 30 days and, for each value, solve the model equations and examine how the eventual amplitude and nadir in neutrophil numbers depends on  $T$ . In our simulations, to study the effects of varying dosage  $D$  and infusion time  $\Delta_c$ , we take  $D = 135$  mg/kg or 175 mg/kg, and  $\Delta_c = 1$  h or 24 h. Results are shown in Fig. 6.

Fig. 6 shows both the amplitude and nadir of simulated neutrophil levels as functions of the chemotherapy period  $T$ . Fig. 6(a) and (b) shows that the numerically determined amplitude has a maximum, and the nadir a minimum, when the period of chemotherapy application is 20 days. The dose of chemotherapy changes the values of the maxima and minima, but does not alter the period at which the maximum amplitude and minimum nadir appear. These results are in accordance with Fig. 6(c) where we show computed time series for the neutrophils at two different periods of chemotherapy administration, indicating that severe neutropenia was produced in the model at  $T = 20$  days but not at  $T = 15$  days. As in Zhuge et al. (2012), the period of 20 days is referred to as the resonant period  $T_R$ , which is approximately twice the average neutrophil life time

$$T_R \approx 2(\tau_N + \gamma_N^{-1}).$$

Note that the amplitude response in Fig. 6(a) has a broad peak at  $T \approx 20$ , and thus a wide range of resonant periods. In contrast, the response function shown by Zhuge et al. (2012) is sharp and therefore the resonant period range is narrow. This width  $\Delta T_R$  in the peak of the response function is important in clinical

treatment in order to decide which periods of chemotherapy to avoid to minimize severe neutropenia. Theoretically,  $\Delta T_R$  is measured by the curvature of the response function at the peak, and therefore is determined by the second derivative of the response function at  $T_R$  (refer to Eq. (C.7)). An analysis in Appendix C indicates that  $\Delta T_R$  is determined by the recovery rate after a single application of chemotherapy discussed above as  $\Delta T_R \propto \alpha^{3/2}$  where  $\alpha$  is the recovery rate. Fig. 7 shows how  $\Delta T_R$  varies with the recovery rate  $\alpha$  when  $s_1$  is varied from 0.1 to 1.0 and other parameters as in Table 1, which gives

$$\text{Resonance width} \approx 44.64 \times \text{recovery rate}^{3/2}, \quad (23)$$

in agreement with our theoretical result. Eq. (23) provides a method to clinically estimate the width of the resonant period peak.

In these simulations, we have chosen parameters consistent with the available data for a hematologically normal individual. However, for a particular patient, there may be inter-individual variation in some of these parameters and we unfortunately have little if any information about this variation. For example, extremely high levels of the absolute neutrophil count before chemotherapy have been reported in some cancer patients (for example,  $41.2 \times 10^8$  cells/kg in Fetterly et al. (2008), and  $74 \times 10^8$  cells/kg in Shankar et al. (2006), 10-fold higher than the normal level) which may indicate activation of immune responses. Here, we adjust the parameters  $\eta_{NP}$ ,  $\gamma_S$  and  $\gamma_0$  (all relate to cell apoptosis rates) to mimic these abnormally high neutrophil levels, and investigate how these changes would then affect the neutrophil response to periodic chemotherapy.

The results are shown in Fig. 8(a), which shows a similar response curve as the default situation given in Fig. 6. Again, there is a resonant period at about  $T = 20$  days.

Next, we examine the effect of changing in  $\kappa_\delta$  on the neutrophil response to periodic chemotherapy. From Fig. 5, an increase in  $\kappa_\delta$  can induce significant changes in the neutrophil response to a short

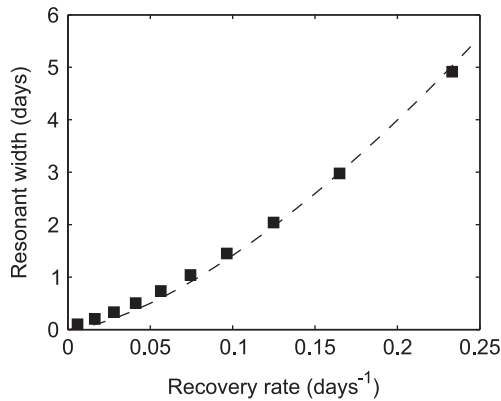


**Fig. 7.** Numerical results for the variation of the resonant period width as a function of the recovery rate  $\alpha$  after a single application of chemotherapy. Computed data are obtained from the response function with the cooperative coefficient  $s_1$  ranging from 0.1 to 1.0. The dashed line shows the fit of Eq. (23) to the computed values. Refer to Appendix C for details. (For interpretation of the references to color in this figure caption, the reader is referred to the web version of this article.)

term application of chemotherapy with period  $T = 21$  days. Fig. 8(b) shows the neutrophil response when  $\kappa_\delta = 0.145$ , with different periods of the periodic chemotherapy. There is a large difference in the response when comparing the results in Fig. 7 with Fig. 8(b). In this case, severe neutropenia always occurs when the period  $T$  varies from 5 to 30 days. However, it is also the case that a maximum neutrophil amplitude (and also the minimum nadir level) occurs when the period  $T$  is about 20 days. The complicated response may originate from the coupling interaction between the periodic perturbation due to chemotherapy and the intrinsic oscillation, but a mathematical understanding awaits further study.

### 3.4. Effects of G-CSF in conjunction with chemotherapy

To study the effect of G-CSF along with periodic chemotherapy, we fix the period of chemotherapy at  $T = 21$  days, in accordance with the protocols for many chemotherapy drugs (Skeel et al., 2007), and then vary the day  $T_1$  of G-CSF administration after chemotherapy. We also alter the dosage and the parameter  $V_{\max}$  in the G-CSF dynamics to examine how the pharmacokinetics might shape the response.

Simulations are shown in Fig. 9(a), which illustrate the dependence of the neutrophil nadir on the day of G-CSF administration in each cycle. The response to G-CSF is highly variable. Giving G-CSF either early or late in each chemotherapy cycle is possible to avoid severe neutropenia, and if  $10 \mu\text{g}/\text{kg}$  filgrastim is administered the most beneficial response (in terms of minimizing the neutropenia) occurs when  $T_1 = 5$  days. Nevertheless, there is a wide range of  $T_1$  at

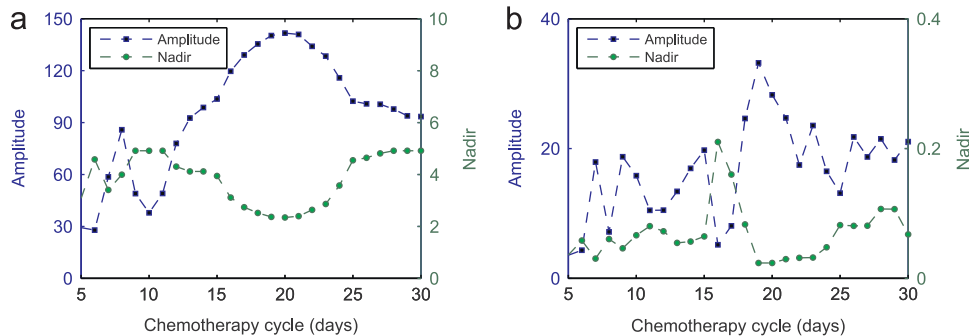


**Fig. 8.** Neutrophil response to periodic administration of chemotherapy with varying period  $T$  and model parameters. Parameters are: (a)  $\eta_{ND} = 2.56$ ,  $\gamma_5 = 0.06$ ,  $\gamma_0 = 0.13$ , and (b)  $\kappa_\delta = 0.145$ , and other parameters as in Table 1 in each case. The chemotherapy dosage  $D = 135 \text{ mg}/\text{kg}$  and the infusion time  $\Delta_c = 1 \text{ h}$  in both cases. In the figure panels, the amplitude (left hand ordinate) in neutrophil response (blue squares connected with a dashed blue line) as well as the nadir (right hand ordinate and green circles connected with a dashed green line) are shown as functions of the period  $T$  of chemotherapy. (For interpretation of the references to color in this figure caption, the reader is referred to the web version of this article.)

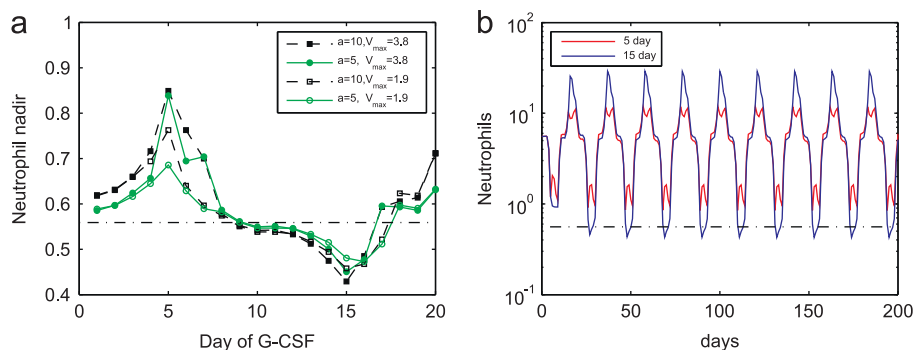


**Fig. 9.** The simulated effect of periodic chemotherapy ( $T = 21$  days) and 1 day G-CSF administration on neutrophil dynamics. Neutrophil levels are in units of  $10^8$  cells/kg. (a) Dependence of the neutrophil nadir on the day of G-CSF administration [filgrastim,  $10 \mu\text{g}/\text{kg}$  (black squares) or  $5 \mu\text{g}/\text{kg}$  (green circles), and  $V_{\max} = 3.8$  (solid) or  $V_{\max} = 1.9$  (hollow) for each case] after chemotherapy in each cycle. (b) Simulated neutrophil response with one day G-CSF ( $10 \mu\text{g}/\text{kg}$  filgrastim) administration 5 or 15 days after chemotherapy, respectively. Dashed-dot lines show the threshold for severe neutropenia ( $0.56 \times 10^8$  cells/kg). In our simulations, the dosage of chemotherapy is  $D = 135 \text{ mg}/\text{kg}$ , and the infusion time is  $\Delta_c = 1 \text{ h}$  at each administration. (For interpretation of the references to color in this figure caption, the reader is referred to the web version of this article.)

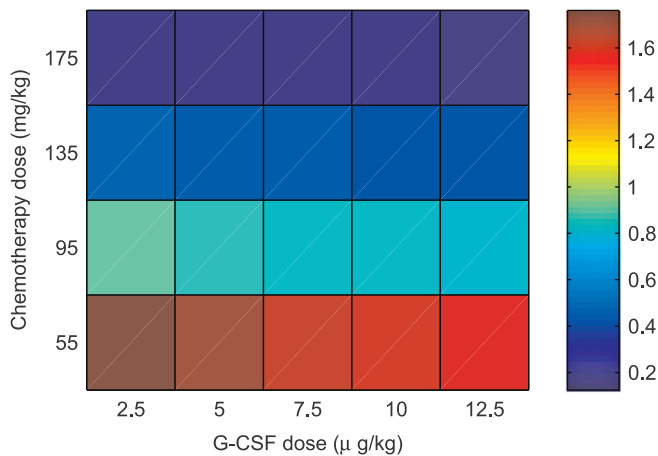


**Fig. 10.** Simulation of the dependence of the nadir in neutrophil levels on doses of chemotherapy and G-CSF. In the simulations, the chemotherapy is administered with a dosage varying from 55 to 175 mg/kg, at a period of 21 days, and the infusion time  $\Delta_c = 1$  h at each administration. The G-CSF dosage varies from 2.5 to 12.5, with the parameter  $V_{\max} = 3.8$ , and G-CSF is administered 15 days after chemotherapy to mimic the *worst* situation.

the middle of each chemotherapy cycle (about 15 days after chemotherapy) that can actually *augment* the neutropenia induced by the chemotherapy. These results are insensitive to either the neutrophil maturation time after G-CSF (controlled by the parameter  $V_{\max}$  in our simulations) or the dosage of G-CSF (Fig. 9a). These observations agree with our previous conclusions obtained with a simpler model (Zhuge et al., 2012). A mathematical analysis that gives a rough understanding of the simulation results is given in Appendix D. Two representative computed neutrophil time series with  $10\mu\text{g/kg}$  filgrastim (and  $V_{\max} = 3.8$ ) administered at either 5 or 15 days after chemotherapy are shown in Fig. 9b. Administering G-CSF 5 days after chemotherapy is able to abolish neutropenia, but G-CSF 15 days after chemotherapy actually *worsens* the neutropenia (compare with Fig. 6)! This result is consistent with clinical observations of a group of metastatic breast cancer patients, that an optimal G-CSF support schedule for alleviating neutropenia is 6–7 days post-docetaxel, administered tri- and bi-weekly (Vainstein et al., 2005a). These results indicate that the timing of G-CSF after chemotherapy is crucial for a positive outcome.

To further investigate how the combination of dosages for chemotherapy and G-CSF shapes the neutrophil response, we simulate the model equations by varying the dosages but fixed the period of chemotherapy and the day of G-CSF unchanged (Fig. 10). The simulations show that the nadir neutrophil level is more sensitive to the dosage of chemotherapy than to that of G-CSF. Thus, a proper dosage of chemotherapy is important for neutrophil response to G-CSF as a post-chemotherapy treatment.

#### 4. Discussion

Before discussing the implications of the present work, a bit of history is in order. Mathematical modeling in biology, indeed in any of the sciences, is a combination of science with a type of ‘art form’. Models are constructed based questions asked, on the biology as well as on observations, available data, and/or data that may be collected. Mathematical models for granulopoiesis have been developed for a number of years, no doubt because of the interesting dynamics that are displayed in some types of pathological hematological states (e.g. cyclical neutropenia). The mathematical formulation of these models varies from group to group depending on individual taste and the questions of interest. Some of the earliest of these are to be found in Wheldon et al.

(1974), Wheldon (1975), MacDonald (1978), Steinbach et al. (1979), Steinbach et al. (1980) and these were compartmental models partially based on the morphological classification of neutrophil precursors. These types of models have been greatly extended by Wichmann and Loeffler (1985) and then used very effectively to examine the hematopoietic response to G-CSF by Schmitz et al. (1993), Schmitz et al. (1996), Shochat et al. (2007), Shochat and Rom-Kedar (2008) and to chemotherapy by Engel et al. (2004), Fetterly et al. (2008). In a long and comprehensive study, Scholz et al. (2005) modified the original Wichmann and Loeffler (1985) formulation to examine granulopoiesis in the face of poly-chemotherapy with G-CSF as an adjunct. In Shochat and Rom-Kedar (2008) the authors study G-CSF effects on chemotherapy-induced neutropenia by expanding a simple mathematical model in Shochat et al. (2007), and the results clarified and complemented the American Society of Clinical Oncology recommendations for G-CSF administration in neutropenia: high sustained G-CSF levels are needed to treat severe neutropenia.

A different modeling approach was taken by Rubinow and Lebowitz (1975) who developed a ‘time-age-maturation’ model for granulopoiesis that has served as a philosophical basis for much of the work done by our group over the past 30 years. This formulation is equivalent at some level to the compartmental approach mentioned above (MacDonald, 1989). In addition to the work from our group, this approach has also been followed by Østby et al. (2004) who also used the same type of model to examine the effects of chemotherapy (Østby et al., 2003) and combined chemotherapy and G-CSF (Østby et al., 2004). In a very nice and relatively recent study, Vainstein et al. (2005b) have used a hybrid of the compartmental and time-age-maturation approaches to granulopoiesis, including details of the neutrophil precursor cell cycle, to examine the effects of G-CSF.

In Zhuge et al. (2012), the authors investigated neutrophil dynamics in response to periodic chemotherapy and G-CSF with a simple mathematical model. Their results suggested that there is a significant period of chemotherapy delivery that can induce resonance in neutrophil dynamics and neutropenia in the system, and that the response to G-CSF is variable. In this paper, we study a mathematical model combining the model in Zhuge et al. (2012) with chemotherapy and G-CSF dynamics to investigate the role of pharmacokinetics in shaping the responses, as well as what may occur when more realistic treatment schedules are used.

A single application of chemotherapy can produce a damped oscillation in both stem cell and neutrophil levels with an oscillation period of about 3 weeks, and a recovery rate of  $0.074\text{ days}^{-1}$ . These dynamic behaviors are independent of the dosages and infusion time of the chemotherapy administration (Fig. 3). The neutrophil level reaches its maximum and nadir during the first oscillation cycle and with values depend exponentially on the chemotherapy dosage (Fig. 3). Further analysis shows that the recovery rate decreases with the cooperativity coefficient ( $s_1$ ) in the feedback function  $\kappa_N$  regulating the rate of differentiation of stem cells into the neutrophil line. However, the coefficient  $s_1$  is simply a phenomenological parameter, no experimental data is available for the estimation of its value, and further clinical justification is required.

With a few (less than five) applications of chemotherapy, the neutrophil dynamics evolve to a stationary state of either constant numbers or permanent oscillation depending on the model parameters and numbers of chemotherapy administrations. Using the parameters as in Table 1 for normally healthy individuals, a finite number of applications of chemotherapy never induces permanent oscillations in neutrophil dynamics, regardless of the dosage or the number of applications of chemotherapy. However, these results are different when the differentiation rate  $\kappa_\delta$  is 10-fold higher ( $\kappa_\delta = 0.145$ ) than the default value. Then, the



model exhibits multi-stability with a co-existence of a stable oscillation and a steady state solution. In this case, if only one chemotherapy is applied, the neutrophil dynamics recover to the normal level after the chemotherapy is stopped. However, if three or more chemotherapy cycles are applied, it can induce permanent oscillations even after the chemotherapy is stopped (Fig. 5).

If periodic chemotherapy is given, we confirmed the observation from Zhuge et al. (2012) that there is a significant resonant period of chemotherapy delivery that induces large amplitude oscillations in neutrophils and subsequent neutropenia (Fig. 6). The width of the resonant period (curvature of the neutrophil response curve with chemotherapy period) is found to increase with the recovery rate of neutrophil levels after a single chemotherapy application. This provides a method to clinically estimate the width of the resonant period peak. Thus, together with the method to estimate the resonant period (twice the average neutrophil lifetime) as has been discussed in Zhuge et al. (2012), it is possible to estimate the period of chemotherapy to avoid possible resonance in neutrophil dynamics. These results are independent of pharmacokinetic parameters of chemotherapy, and remain valid when apoptosis rates are reduced abnormally. Increasing the differential rate  $\kappa_\delta$  may result in a different profile of the neutrophil amplitude response function with the chemotherapy period, but the significant effect of resonance remain unaffected (Fig. 8).

If chemotherapy is given at a period  $T$  in combination with G-CSF  $T_1$  days later then the results depend on the day of G-CSF administration. When the chemotherapy is delivered at a period of 3 weeks (as suggested for many chemotherapy drugs), there is a range of  $T_1$  values (either early or late in each chemotherapy cycle) such that G-CSF administration has positive effects in eliminating severe neutropenia (Fig. 9). However, there is also a range of  $T_1$  (around 15 days after chemotherapy) that will lead to a worsening by G-CSF of the neutropenia induced by the chemotherapy (Fig. 9). These results are independent of the G-CSF dosage and qualitatively in agreement with the results presented in Zhuge et al. (2012), but await confirmation from clinical observations.

In Zhuge et al. (2012) and the current study, only the neutrophil response to chemotherapy was considered and the platelet and red blood cell responses that have been reported (Sola et al., 2000) were not treated. These responses can be important for an understanding of the full hematopoietic response and also for

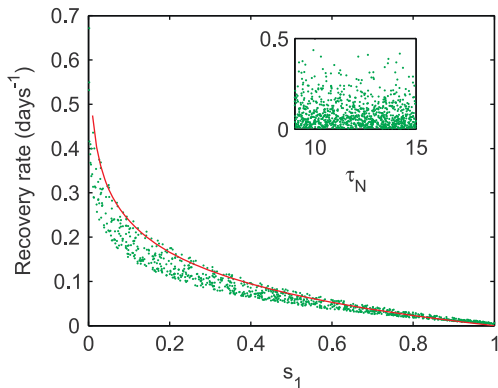


**Fig. 11.** Numerical solutions of the dependence of the recovery rate  $\alpha$  on the cooperativity coefficient  $s_1$  and  $\tau_N$  (inset). The recovery rate is given by the maxima negative real parts of the root of  $h(s) = 0$ . In simulations, we change  $0 < s_1 < 1$  and  $9 < \tau_N < 15$  randomly and independently uniformly distributed over the intervals, and adjust  $\theta_1$  according to (C.4), and kept the other parameters unchanged from their values in Table 1. Red solid line shows the curve  $\alpha = \tau_N^{-1} \ln s_1$  with  $\tau_N = 9.7$  days as in Table 1. (For interpretation of the references to color in this figure caption, the reader is referred to the web version of this article.)

predicting the effect of G-CSF administration. A more comprehensive model of the entire hematopoietic system is needed to further investigate the response of chemotherapy and G-CSF. Although clinicians have recognized the connection between the timing of chemotherapy and the development of neutropenia, as far as we are aware, the work by Zhuge et al. (2012) and the current paper are the first to illuminate the potential for destructive resonance leading to neutropenia in response to periodic chemotherapy, and to systematically explore and explain why the timing of G-CSF is so crucial for successful reversal of chemotherapy induced neutropenia.

## Acknowledgments

This work was supported by the Natural Sciences and Engineering Research Council (NSERC, Canada), and the Mathematics of Information Technology and Complex Systems (MITACS, Canada), and the National Natural Science Foundation of China (NSFC 10971113, China), and carried out in Montréal and Beijing. We thank our colleagues C. Zhuge, J. Bélair, T. Humphries and Loic Ferraton for valuable discussions and support. GB thanks C. Zhuge for helping in programming. We are indebted to two referees for valuable comments on the first submission of this paper that helped to substantially improve it.

## Appendix A. Saturable clearance of G-CSF

The saturable clearance of G-CSF,  $F(G)$ , can be derived by examining the interaction between G-CSF and the G-CSF receptor as below. From Layton and Hall (2006), at least two G-CSF molecules bind to a single G-CSF receptor. The resulting G-CSF/receptor complex is internalized and the G-CSF molecule is degraded, after which the receptor is released. We write these processes as:



which gives the rates of change for concentrations of G-CSF ( $[G]$ ) and G-CSF/receptor complex ( $[RG_2]$ ) as

$$\frac{d[G]}{dt} = -k_1[R][G]^2 + k_{-1}[RG_2] \quad (A.2)$$

$$\frac{d[RG_2]}{dt} = k_1[R][G]^2 - (k_{-1} + k_2)[RG_2]. \quad (A.3)$$

We assume the internalization of the G-CSF/receptor complex is fast once G-CSF molecules bind to the receptor, and therefore  $[RG_2]$  is at the state of quasi-equilibrium so that Eq. (A.3) reduces to

$$[RG_2] = \frac{k_1}{k_{-1} + k_2} [R][G]^2. \quad (A.4)$$

Let  $k = (k_{-1} + k_2)/k_1$ . Since the total concentration of receptors equal the total concentration of neutrophil  $[N]$  times the average number  $n$  of receptors per neutrophil, we have

$$[R] = n[N] - [RG_2],$$

and thus we obtain

$$[RG_2] = \frac{n[N][G]^2}{k + [G]^2}. \quad (A.5)$$

Substituting Eqs. (A.4) and (A.5) into Eq. (A.2), we finally obtain

$$\frac{d[G]}{dt} = -k_2 \frac{n[N][G]^2}{k + [G]^2}. \quad (A.6)$$

Thus, comparing with (11) and dropping the bracket notation, we have

$$F(G) = \frac{G^2}{k+G^2} \quad (\text{A.7})$$

and  $\sigma = k_2 n$ .

## Appendix B. Parameter estimation

A number of studies have provided estimations for the parameters of this model, and readers are referred to Bernard et al. (2003); Foley and Mackey (2009); Lei and Mackey (2011); Zhuge et al. (2012)). Parameters used in the current study are summarized in Table 1 and are detailed below.

### B.1. Hematological model parameters

Estimation of the parameters is crucial in order to obtain physiologically reasonable parameters. In general, some of the parameters can be retrieved or be derived from experimental data found in the literature, or derived from the steady-state solutions of equations (1) and (2).

The steady state value of the stem cells in the resting phase ( $G_0$  phase),  $Q_*$ , is estimated from different sets of experimental data on the numbers of stem cells per nucleated bone marrow cells in mice and cats. Boggs et al. (1982), Micklem et al. (1987), Harrison et al. (1988), McCarthy (1997) gave a value that varies from 1 to 50 stem cells per  $10^5$  nucleated bone marrow cells in mice, whereas Abkowitz et al. (2000) gave a value of eight stem cells per  $10^5$  nucleated bone marrow cells in cats. Novak and Nečas (1994) gave a mean count of  $1.4 \times 10^{10}$  nucleated bone marrow cells per kg in mice. Since the number of stem cells per nucleated bone marrow cells seem somewhat similar between both mice and cats, we can estimate from the two previous experimental results that

$$Q_* = (8/10^5) \times 1.4 \times 10^{10} = 1.12 \times 10^6 \text{ cells/kg.} \quad (\text{B.1})$$

We infer  $\gamma_S$ , the apoptosis rate of HSC, and  $\tau_S$ , the time for the stem cell to divide during the proliferation phase, from Mackey (2001), i.e.,  $\gamma_S = 0.1043 \text{ days}^{-1}$  and  $\tau_S = 2.83 \text{ days}$ , respectively. Bernard et al. (2003a) found that the value of  $k_0 = 8.0 \text{ days}^{-1}$  in the stem cell reentry rate ( $\beta(Q_*)$ ) gave a good fit to the experimental data of Oostendorp et al. (2000). It is not clear what the value of  $s_2$ , the cooperativity coefficient of the stem cell reentry rate, should be (Bernard et al., 2003a). There is evidence that at least two different cytokines are needed to trigger HSC proliferation *in vitro*, and so we take the value of  $s_2$  to be equal to 2. The last parameter of the stem cell reentry rate,  $\theta_2$ , is calculated from the experimental steady state value of  $\beta(Q_*)$  and the above parameters. From Mackey (2001), we have calculated the average of  $\beta(Q_*)$  of the mice data to be 0.04333. It is then straightforward to compute the value of  $\theta_2$  to be  $0.0826 \times 10^6 \text{ cells/kg}$ .

The total differentiation rate of the platelet and erythrocyte lines,  $\kappa_\delta$ , is assumed to be a constant and equal to  $0.0134 \text{ days}^{-1}$ . The value is calculated from various experimental results and estimations (Colijn and Mackey, 2005b; Lei and Mackey, 2011).

Hearn et al. (1998) found  $\tau_N = 9.7 \text{ days}$  and  $\tau_{NM} = 3.8 \text{ days}$  following analysis of data from Perry et al. (1966), which in turn gives 5.9 days for  $\tau_{NP}$ , a value in agreement with a value of 6.0 days quoted by Israels and Israels (2002). The random loss rate of neutrophils in the circulation,  $\gamma_N$ , has been estimated by Haurie et al. (2000) to be  $2.4 \text{ days}^{-1}$ . The amplification parameter  $A_N$  is then calculated from the other parameters and the constraint that at steady state Eqs. (1) and (2) are equal to 0. Indeed, we can solve  $A_N$  from the other parameters in Eq. (2), and then by solving for

$\kappa(N_*)$  in Eq. (1) and substituting in Eq. (2):

$$\begin{aligned} A_N &= (\gamma_N N_*) / (\kappa_N(N_*) Q_*) \\ &= (\gamma_N N_*) / (Q_* (\beta(Q_*) (2e^{-\gamma_S \tau_S} - 1) - \kappa_\delta)) \\ &\approx 1549.58. \end{aligned} \quad (\text{B.2})$$

The normal death rate of proliferative neutrophil precursors,  $\gamma_0$ , is set to  $0.27 \text{ days}^{-1}$ . Given  $A_N = e^{\eta_{NP} \tau_{NP} - \gamma_0 \tau_{NM}}$ , we can solve for the proliferation rate of neutrophil precursors,  $\eta_{NP}$ , and obtain  $\eta_{NP} = 2.1995 \text{ days}^{-1}$ . Some experiments report a 20-fold increase in differentiation activity under administration of G-CSF (Bernard et al., 2003a and references therein). This suggests that the maximal differentiation activity under administration of G-CSF is  $f_0 \approx 20 \times \kappa_N(N_*) = 20 \times (\gamma_N N_*) / (A_N Q_*) = 0.154605 \text{ days}^{-1}$ . Bernard et al. (2003a) assumed the cooperativity coefficient  $s_1$  of the feedback function of neutrophils to be 1. However, this value results in a long recovery time after one chemotherapy injection that is clinically unrealistic. In this study, we chose the cooperativity coefficient  $s_1 = 0.5$  (see Appendix C), and therefore  $\theta_1$  is calculated to be  $0.0154848 \times 10^8 \text{ cells/kg}$  from the condition that Eq. (2) is equal to 0 at steady state.

### B.2. Chemotherapy

In the chemotherapy kinetics, we chose to use a value of  $\delta = 100 \text{ days}^{-1}$ , corresponding to a decay time of  $0.24 \text{ h}^{-1}$ . This value is approximately the decay time for a number of relatively common chemotherapy drugs, including Taxol (Henningsson et al., 2001), Carboplatin (Oguri et al., 1988), Gemcitabine (Kiani et al., 2003), and several others.

To mimic the role of chemotherapy, we need to know how chemotherapy drugs affect the cell apoptosis rates, i.e., the coefficients  $h_S$  and  $h_{NP}$  in (8) and (9). However, there is no good experimental evidence that qualitatively connects the plasma concentration of chemotherapy drugs with cell apoptosis rates. Referring to previous studies (Foley and Mackey, 2009; Zhuge et al., 2012), we take the maximum apoptosis rate  $\gamma_S^{\text{max}} = 0.4 \text{ day}^{-1}$  and minimum proliferation rate  $\eta_{NP}^{\text{min}} = 0.4 \text{ day}^{-1}$ , to represent the effect of one day chemotherapy administration. These number are taken so that the model displays neutropenia. Here, we refer to these values as our baseline, and assume that they correspond to a 1 day infusion of 135 mg/kg chemotherapy drug, i.e.,  $D = 135 \text{ mg/kg}$ , and  $\Delta_c = 1 \text{ day}$ , and hence  $I_0 = 135 \text{ mg}/(\text{kg} \times \text{day})$ .

From (8), the total cell loss in the stem cell compartment during the first day of drug injection (normalized by the total loss in stem cell number, which is assumed to be a constant, i.e.,  $S(t) \equiv S_0$  when  $0 \leq t \leq 1$ ) is given by

$$\begin{aligned} L_S &= \int_0^1 \gamma_S^{\text{chemo}}(t) S(t) dt / \int_0^1 S(t) dt \\ &= S_0 \int_0^1 \gamma_S^{\text{chemo}}(t) dt / S_0 \\ &= \gamma_S + h_S \int_0^1 C(t) dt \\ &= \gamma_S + h_S (I_0 / \phi) (1 - \delta^{-1} (1 - e^{-\delta})) \\ &\approx \gamma_S + h_S I_0 / \phi. \end{aligned}$$

Here we note  $\Delta_c = 1$  and  $\delta = 100 \gg 1$ . We compare  $L_S$  with the above  $\gamma_S^{\text{max}}$  ( $\times 1 \text{ day}$ ), which also gives the total loss in stem cell number during 1 day of drug injection. Thus, we should have

$$\gamma_S^{\text{max}} = \gamma_S + h_S I_0 / \phi,$$

which yields

$$h_S = \phi (\gamma_S^{\text{max}} - \gamma_S) / I_0 = \phi (\gamma_S^{\text{max}} - \gamma_S) / 135 = 0.0702 \text{ kg}/(\text{mg} \times \text{day}). \quad (\text{B.3})$$

Similarly, we have

$$h_{NP} = \phi(\eta_{NP} - \eta_{NP}^{\min})/135 = 0.4275 \text{ kg}/(\text{mg} \times \text{day}). \quad (\text{B.4})$$

### B.3. G-CSF administration

Parameters for the G-CSF administration are taken from the filgrastim data in [Foley and Mackey \(2009\)](#), with changes detailed below. The amplification rate in neutrophil development is defined as

$$A_N = e^{\tau_{NP}\eta_{NP} - \gamma_0\tau_{NM}}.$$

After G-CSF administration, the apoptosis rate of maturing neutrophil precursors decreases to  $\gamma_0^{\min} = 0.12$ , and the amplification rate can be increased to  $2^{21}$ . Therefore, the maximum proliferation rate  $\eta_{NP}^{\max}$  is given by

$$\eta_{NP}^{\max} = (\ln A_N^{\max} + \gamma_0^{\min}\tau_{NM})/\tau_{NP} = 2.5444 \text{ days}^{-1}. \quad (\text{B.5})$$

## Appendix C. Recovery rate and the resonance period width

To obtain the relationship between the recovery rate, the resonance period width, and the cooperative coefficient  $s_1$ , we first simplify the model equation, and then study the response function as in [Zhuge et al. \(2012\)](#).

We assume HSC numbers to be held constant ( $Q(t) \equiv Q_*$ ) and therefore have a single equation for the neutrophil dynamics

$$dN/dt = -\gamma_N N + A_N \kappa_N(N_{\tau_N}) Q_*. \quad (\text{C.1})$$

In [Zhuge et al. \(2012\)](#), Eq. (C.1) was used to study the neutrophil compartment dynamics and gave significant insight for the full model.

Linearization of Eq. (C.1) near the steady state  $N(t) = N_*$  prior to chemotherapy gives following characteristic equation

$$h(s) = s + \gamma_N + B e^{-s\tau_N} \quad (\text{C.2})$$

where

$$B = -A_N Q_* \kappa'_N(N_*) = \gamma_N s_1 N_*^{s_1} / (\theta_1^{s_1} + N_*^{s_1}). \quad (\text{C.3})$$

Let  $\hat{s} = -\alpha + i\beta$  be the root of  $h(s) = 0$  with the maximum real part (which is negative), then  $\alpha$  gives the recovery rate after a single dose of chemotherapy.

From Eqs. (C.2)–(C.3), the recovery rate depends on  $\gamma_N, \tau_N, s_1, \theta_1$  and  $N_*$ , and two of them ( $s_1$  and  $\theta_1$ ) are connected by

$$\kappa_N(N_*) = \gamma_N N_* / (A_N Q_*). \quad (\text{C.4})$$

From [Appendix B.1](#), the parameter values of  $\gamma_N, N_*, Q_*$  and  $A_N$  are relatively precise from a variety of experimental data, a range of  $9 < \tau_N < 14.4$  is suggested according to [Price et al. \(1996\)](#), and  $s_1$  is the most problematic. [Fig. 11](#) shows the dependence of the recovery rate  $\alpha$  on  $s_1$  and  $\tau_N$ . It is obvious that the recovery rate decreases with  $s_1$ , and is insensitive to  $\tau_N$ .

In order to obtain an approximate relation between  $\alpha$  and  $s_1$ , we substitute  $s = -\alpha + i\beta$  to Eq. (C.2) to obtain

$$\beta - B e^{\alpha\tau_N} \sin(\beta\tau_N) = 0.$$

Therefore,

$$\alpha = (\log(\beta/\sin \beta\tau_N) - \log B) / \tau_N.$$

Here  $\beta$  is close to the resonant frequency and is given approximately  $\beta \approx \pi / (\tau_N + \gamma_N^{-1})$  from the discussion in [Zhuge et al. \(2012\)](#). From Eqs. (C.3) and (C.4), we have

$$B = \gamma_N s_1 (1 - \gamma_N N_* / (f_0 A_N Q_*)).$$

Hence, we have approximately

$$\alpha = -\tau_N^{-1} \ln(s_1/A) \quad (\text{C.5})$$

where  $A = (B \sin \beta\tau_N) / (\beta s_1)$  is independent of  $s_1$ . For parameters in [Table 1](#), we have approximately  $A=1$  (see [Fig. 11](#)).

Now, we find the connection between the recovery rate and the resonance period width. From Eq. (A.4) in [Zhuge et al. \(2012\)](#), the frequency response function of Eq. (C.1) at  $N(t) = N_*$  is given by

$$F(\omega) = |\kappa_N(N_*) Q_* / h(i\omega)|. \quad (\text{C.6})$$

The resonant frequency  $\omega_R$  is obtained by maximizing  $F(\omega)$ , i.e., minimizing  $|h(i\omega)|$ . The resonance period width is measured by the second derivative of the response function at  $\omega_R$  as following

$$\Delta T_R = \sqrt{|1/F''(\omega_R)|}. \quad (\text{C.7})$$

We note  $h(\hat{s}) = 0$  and hence

$$h(i\omega) \approx c(i\omega - \hat{s})$$

when  $i\omega \approx \hat{s} = -\alpha + i\beta$ , where  $c$  is a coefficient independent of  $\omega$ . Therefore when  $\alpha$  is small,

$$F(\omega) \approx |\kappa_N(N_*) Q_* / (c(i\omega + \alpha - i\beta))|,$$

which yields the resonant frequency  $\omega_R = \beta$ , and when  $\omega \approx \beta$

$$F(\omega) \approx c_0 (1/\alpha - (\omega - \beta)^2 / (2\alpha^3)) \quad (\text{C.8})$$

where  $c_0 = |\kappa_N(N_*) Q_* / c|$ . Therefore, the resonance period width is calculated to be

$$\Delta T_R = \sqrt{\alpha^3 / c_0} \text{ (days)}. \quad (\text{C.9})$$

Eq. (C.9) gives the fit for [Fig. 7](#).

## Appendix D. Understanding the effect of G-CSF timing

In Eq. (C.1), the combined chemotherapy plus G-CSF administration is a periodic perturbation with period  $T$  of the amplification factor so  $A_N(t)$  can be expressed as  $A_N(t) = A_N + \zeta(t)$ , where  $A_N$  is the normal amplification rate and  $\zeta(t)$  the periodic perturbation due to the combined chemotherapy and G-CSF therapy. Linearization of (C.1) near the steady state  $N_*$  gives the linear differential delay equation

$$dy/dt = -\gamma_N y - B y_{\tau_N} + \zeta(t) \kappa_N(N_*) Q_*, \quad (\text{D.1})$$

where  $B$  is given in [C.3](#). Write  $\zeta(t) = \zeta_G(t) - \zeta_C(t)$  where  $\zeta_G(t)$  and  $\zeta_C(t)$  are, respectively, the periodic perturbations due to G-CSF and chemotherapy. Given  $\zeta_C(t)$ , the function  $\zeta_G(t)$  depends on the G-CSF delivery protocol, and the relation between these two functions are complicated. Here, we perform the analysis by simply assuming the input functions satisfy

$$\zeta_G(t) = r \zeta_C(t - T_e) \quad (\text{D.2})$$

where  $r$  is a constant and  $T_e$  is the lag time between G-CSF and chemotherapy to become effective in perturbing the amplification rate  $A_N$ . Because of the postponed response of chemotherapy (see [Section 3.1](#)),  $T_e$  is usually not the same as  $T_1$ , the day of G-CSF administration after chemotherapy.

Let  $\hat{f}(s)$  be the Laplace transform of  $f(t)$ , defined as

$$\hat{f}(s) = \int_0^\infty e^{-st} f(t) dt,$$

and take the Laplace transform of Eq. (D.1) to give

$$H(s) = \hat{y}(s) / \hat{\zeta}_C(s) = H_1(s) \cdot H_2(s)$$

where

$$H_1(s) = -\kappa(N_*) Q_* / (s + \gamma_N + B e^{-s\tau_N}),$$

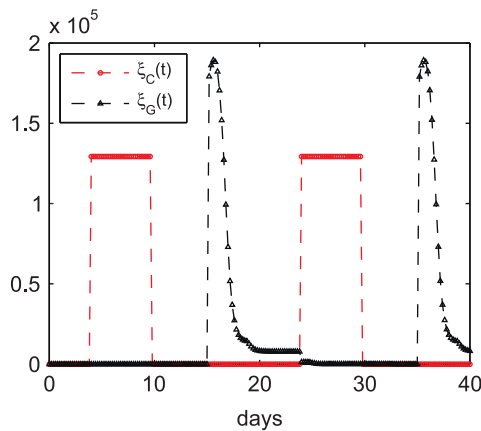


**Fig. 12.** Perturbation  $\xi_C(t)$  and  $\xi_G(t)$  to the amplification rate. Here the period  $T = 20$  days and  $\xi_C(t)$  is calculated with  $T_1 = 15$  days.

$$H_2(s) = 1 - re^{-sT_e}$$

Thus, the transfer function for Eq. (C.1) is given by

$$F(\omega) = |H(i\omega)| = |H_1(i\omega)| \cdot |H_2(i\omega)|. \quad (\text{D.3})$$

If we have chosen the period  $T$  of chemotherapy and G-CSF administration to coincide with the resonant period of  $|H_1(i\omega)|$  then the response to the G-CSF will be determined by the behavior of

$$|H_2(i\omega)| = 1 - 2r \cos(\omega T_e) + r^2. \quad (\text{D.4})$$

This function will have a maximum when  $T_e = T/2$ .

In this study, the resonant period is  $T = 20$  days, so we expect that the worst outcome from G-CSF would occur when  $T_e = T/2 = 10$  days. Since the amplification rate  $A_N$  responds to chemotherapy with a delay of 5 days, and to G-CSF without delay (Fig. 12), the value  $T_e = 10$  is reached when G-CSF is administered around 15 days after chemotherapy. Fig. 12 shows the functions  $\xi_C(t)$  and  $\xi_G(t)$  with  $T_1 = 15$  days, which gives  $T_e = 10$  days. This provides a rough understanding for the effect of G-CSF timing in Section 3.4.

## References

Abkowitz, J.L., Golinelli, D., Harrison, D.E., Guttorp, P., 2000. In vivo kinetics of murine hemopoietic stem cells. *Blood* 96, 3399–3405.

Andersen, L.K., Mackey, M.C., 2001. Resonance in periodic chemotherapy: a case study of acute myelogenous leukemia. *J. Theor. Biol.* 209, 113–130.

Bernard, S., Pujol-Menjouet, L., Mackey, M.C., 2003a. Analysis of cell kinetics using a cell division marker: mathematical modeling of experimental data. *Biophys. J.* 84, 3414–3424.

Bernard, S., Bélair, J., Mackey, M.C., 2003. Oscillations in cyclical neutropenia: new evidence based on mathematical modeling. *J. Theor. Biol.* 223, 283–298.

Boggs, D., Boggs, S., Saxe, D., Gress, L., Canfield, D., 1982. Hematopoietic stem cells with high proliferative potential assay of their concentration in marrow by the frequency and duration of cure of W/W<sup>v</sup> mice. *J. Clin. Invest.* 70, 242–253.

Butler, R.D., Waites, T.M., Lamar, R.E., Hainsworth, J.D., Greco, F.A., Johnson, D.H., 1992. Timing of G-CSF administration during intensive chemotherapy for breast cancer (abstract). *Am. Soc. Clin. Oncol.* 11, 1411.

Colijn, C., Mackey, M.C., 2005a. A mathematical model of hematopoiesis: I periodic chronic myelogenous leukemia. *J. Theor. Biol.* 237, 117–132.

Colijn, C., Mackey, M.C., 2005b. A mathematical model of hematopoiesis: II. Cyclical neutropenia. *J. Theor. Biol.* 237, 133–146.

Colijn, C., Foley, C., Mackey, M.C., 2007. G-CSF treatment of canine cyclical neutropenia: a comprehensive mathematical model. *Exp. Hematol.* 37, 898–907.

Crawford, J., Dale, D.C., Lyman, G.H., 2003. Chemotherapy-induced neutropenia: risks, consequences, and new directions for its management. *Cancer* 100, 228–237.

Dale, David C., Alling, David W., Wolff, Sheldon M., 1973. Application of time series analysis to serial blood neutrophil counts in normal individuals and patients receiving cyclophosphamide. *Br. J. Haematol.*, 24(1), 57–64.

Dancey, J.T., Deubelbeiss, K.A., Harker, L.A., Finch, C.A., 1976. Neutrophil kinetics in man. *J. Clin. Invest.* 58, 705–715.

Engel, C., Scholz, M., Loeffler, M., 2004. A computational model of human granulopoiesis to simulate the hematotoxic effects of multicycle polychemotherapy. *Blood* 104 (8), 2323–2331.

Fetterly, Gerald J., Grasela, Thaddeus H., Sherman, Jeffrey W., Dul, Jeanne L., Grahn, Amy, Lecomte, Diane, Fiedler-Kelly, Jill, Damjanov, Nevena, Fishman, Mayer, Kane, Michael P., Rubin, Eric H., Tan, Antoniette R., 2008. Pharmacokinetic/pharmacodynamic modeling and simulation of neutropenia during phase 1 development of liposome-entrapped Paclitaxel. *Clin. Cancer Res.* 14, 5856–5863.

Fogli, S., Danesi, R., Braud, F. De, Pas, T. De, Curigliano, G., Giovannetti, E., Tacca, M. Del. 2001. Drug distribution and pharmacokinetic/pharmacodynamic relationship of paclitaxel and gemcitabine in patients with non-small-cell lung cancer. *Ann. Oncol.* 12, 1553–1559.

Foley, C., Mackey, M.C., 2009. Mathematical model for G-CSF administration after chemotherapy. *J. Theor. Biol.* 257, 27–44.

Foley, C., Bernard, S., Mackey, M., 2006. Cost-effective G-CSF therapy strategies for cyclical neutropenia: mathematical modelling based hypotheses. *J. Theor. Biol.* 238, 754–763.

Fukuda, M., Nakato, M., Kinoshita, A., et al., 1993. Optimal timing of G-CSF administration in patients receiving chemotherapy for non-small cell lung cancer (NSCLC) (abstract). *Am. Soc. Clin. Oncol.* 12, 1549.

Gianni, L., Kearns, C.M., Gianni, A., Capri, G., Viganò, L., Locatelli, A., Bonadonna, G., Egorin, M.J., 2011. Nonlinear pharmacokinetics and metabolism of Paclitaxel and its pharmacokinetic/pharmacodynamic relationships in humans. *J. Clin. Oncol.* 13, 180–190.

Green, M.D., Koelbl, H., Baselga, J., Galid, A., Guillem, V., Gascon, P., Siena, S., Lalisang, R.I., Samonigg, H., Clemens, M.R., Zani, V., Liang, B.C., Renwick, J., Piccart, M.J., 2003. A randomized double-blind multicenter phase III study of fixed-dose single-administration pegfilgrastim versus daily filgrastim in patients receiving myelosuppressive chemotherapy. *Ann. Oncol.* 14, 29–35.

Harrison, D., Astle, C., Lerner, C., 1988. Number and continuous proliferative pattern of transplanted primitive immunohematopoietic stem cells. *Proc. Natl. Acad. Sci. USA* 85, 822–826.

Haurie, C., Dale, D.C., Rudnicki, R., Mackey, M.C., 2000. Modeling complex neutrophil dynamics in the grey collie. *J. Theor. Biol.* 24, 505–519.

Hearn, T., Haurie, C., Mackey, M.C., 1998. Cyclical neutropenia and the peripheral control of white blood cell production. *J. Theor. Biol.* 192, 167–181.

Henningson, A., Karlsson, M.O., Viganò, L., Gianni, L., Verweij, J., Sparreboom, A., 2001. Mechanism-based pharmacokinetic model for paclitaxel. *J. Clin. Oncol.* 19, 4065–4073.

Israels, L.G., Israels, E.D., 2002. Mechanisms in Hematology. Core Health Services Inc.

Karl, S., Häckerand, S., Mader, I., Cristofanon, S., Schweitzer, T., Krauss, J., Rutkowski, S., Debatin, K.-M., Fulda, S., 2011. Histone deacetylase inhibitors prime medulloblastoma cells for chemotherapy-induced apoptosis by enhancing p53-dependent Bax activation. *Oncogene* 30, 2275–2281.

Kennedy, B.J., 1970. Cyclic leukocyte oscillations in chronic myelogenous leukemia during hydroxyurea therapy. *Blood* 35 (6), 751–760.

Kiani, A., Köhne, C.-H., Franz, T., Passauer, J., Haufe, T., Gross, P., Ehninger, G., Schleyer, E., 2003. Pharmacokinetics of gemcitabine in a patient with end-stage renal disease: effective clearance of its main metabolite by standard hemodialysis treatment. *Cancer Chemother. Pharmacol.* 51, 226–270.

Koumakis, G., Vassilomanolakis, M., Barbounis, V., Hatzichristou, E., Demiri, S., Platanoiotis, G., Pamouktsoglou, F., Efrmidis, A., 1999. Optimal timing (pre-emptive versus supportive) of granulocyte colony-stimulating factor administration following high-dose cytophosphamide. *Oncology* 56, 28–35.

Layton, J.E., Hall, N.E., 2006. The interaction of G-CSF with its receptor. *Front. Biosci.* 11, 3181–3189.

Leavey, P.J., Sellins, K.S., Thurman, G., Elzi, D., Hiester, A., Silliman, C.C., Zerbe, G., Cohen, J.J., Ambruso, D.R., 1998. In vivo treatment with granulocyte colony-stimulating factor results in divergent effects on neutrophil functions measured in vitro. *Blood* 92, 4366–4374.

Lei, J., Mackey, M.C., 2011. Multistability in an age-structured model of hematopoiesis: cyclical neutropenia. *J. Theor. Biol.* 270, 143–153.

Levine, M.N., Whelan, T., 2006. Adjuvant chemotherapy for breast cancer—30 years later. *N. Engl. J. Med.* 355, 1920–1922.

MacDonald, N., 1978. Cyclical neutropenia: models with two cell types and two time lags. In: Valleron, A.J., Macdonald, P.D.M. (Eds), *Biomathematics and Cell Kinetics*. Amsterdam: Elsevier/North-Holland, Amsterdam.

MacDonald, N., 1989. *Biological Delay Systems: Linear Stability Theory*. Cambridge University Press, Cambridge.

Mackey, M.C., 2001. Cell kinetic status of hematopoietic stem cells. *Cell Prolif.* 34, 71–83.

McCarthy, K.F., 1997. Population size and radiosensitivity of murine hematopoietic endogenous long-term repopulating cells. *Blood* 89, 834–841.

Meisenberg, B.R., Davis, T.A., Melaragno, A.J., Stead, R., Monroy, R.L., 1992. A comparison of therapeutic schedules for administering granulocyte colony-stimulating factor to nonhuman primates after high-dose chemotherapy. *Blood* 79, 2267–2272.

Merchant, A.A., Singh, A., Matsui, W., Biswal, S., 2011. The redox-sensitive transcription factor Nrf2 regulates murine hematopoietic stem cell survival independently of ROS levels. *Blood* 118 (25), 6572–6579.

Mickleth, H., Lennon, J., Ansell, J., Gray, R.A., 1987. Numbers and dispersion of repopulating hematopoietic cell clones in radiation chimeras as functions of injected cell dose. *Exp. Hematol.* 15, 251–257.

Minkin, P., Zhao, M., Chen, Z., Ouwerkerk, J., Gelderblom, H., Baker, S.D., 2008. Quantification of sunitinib in human plasma by high-performance liquid



- chromatography-tandem mass spectrometry. *J. Chromatogr. B Analyt. Technol. Biomed. Life Sci.* 874, 84–88.
- Morikawa, N., Mori, T., Abe, T., Ghoda, M., Takeyama, M., Hori, S., 1997. Pharmacokinetics of methotrexate in plasma and cerebrospinal fluid. *Ann. Pharmacother.* 31, 1153–1156.
- Morstyn, G., Campbell, L., Lieschke, G., Layton, J.E., Maher, D., O'Connor, M., Green, M., Sheridan, W., Vincent, M., Alton, K., Souza, L., McGrath, K., Fox, R.M., 1989. Treatment of chemotherapy-induced neutropenia by subcutaneously administered granulocyte colony-stimulating factor with optimization of dose and duration of therapy. *J. Clin. Oncol.* 7, 1554–1562.
- Mou, C., Ganju, N., Sridhar, K.S., Krishan, A., 1997. Simultaneous quantitation of plasma doxorubicin and prochlorperazine content by high-performance liquid chromatography. *J. Chromatogr. B* 703, 217–224.
- Novak, J.P., Nečas, E., 1994. Proliferation differentiation pathways of murine haematopoiesis: correlation of lineage fluxes. *Cell. Prolif.* 27, 597–633.
- Oguri, S., Sakakibara, T., Mase, H., Shimizu, T., Ishikawa, K., 1988. Clinical pharmacokinetics of carboplatin. *J. Clin. Pharmacol.* 28 (3), 208–215.
- Oostendorp, R.A., Audet, J., Eaves, C.J., 2000. High-resolution tracking of cell division suggests similar cell kinetics of hematopoietic stem cells simulated in vitro and in vivo. *Blood* 95, 855–862.
- Østby, I., Rusten, L.S., Kvalheim, G., Grøttum, P., 2003. A mathematical model of reconstitution of granulopoiesis after high dose chemotherapy with autologous stem cell transplantation. *J. Math. Biol.* 47, 101–136.
- Østby, I., Kvalheim, G., Rusten, L.S., Grøttum, P., 2004. Mathematical modeling of granulocyte reconstitution after high-dose chemotherapy with stem cell support: effect of posttransplant G-CSF treatment. *J. Theor. Biol.* 231, 69–83.
- Østby, Ivar, Winther, Ragnar. 2004. Stability of a model of human granulopoiesis using continuous maturation. *J. Math. Biol.*, 49(5), 501–536.
- Peng, B., Hayes, M., Resta, D., Racine-Poon, A., Druker, B.J., Talpaz, M., Sawyers, C.L., Rosamilia, M., Ford, J., Lloyd, P., Capdeville, R., 2004. Pharmacokinetics and pharmacodynamics of imatinib in a phase I trial with chronic myeloid leukemia patients. *J. Clin. Oncol.* 22, 935–942.
- Perry, S., Moxley, J.H., Weiss, G.H., Zelen, M., 1966. Studies of leukocyte kinetics by liquid scintillation counting in normal individuals and in patients with chronic myelogenous leukemia. *J. Clin. Invest.* 45, 1388–1399.
- Price, T.H., Chatta, G.S., Dale, D.C., 1996. Effect of recombinant granulocyte colony-stimulating factor on neutrophil kinetics in normal young and elderly humans. *Blood* 88, 335–340.
- Rahman, Z., Esparza-Guerra, L., Yap, H.Y., Fraxchini, G., Bodey, G., Hortobagyi, G., 1997. Chemotherapy-induced neutropenia and fever in patients with metastatic breast carcinoma receiving salvage chemotherapy. *Cancer* 79, 1150–1157.
- Rubinow, S., Lebowitz, J., 1975. A mathematical model of neutrophil production and control in normal man. *J. Math. Biol.* 1, 187–225.
- Schmitz, S., Franke, H., Brusis, J., Wichmann, H.E., 1993. Quantification of the cell kinetic effect of G-CSF using a model of human granulopoiesis. *Exp. Hematol.* 21, 755–760.
- Schmitz, S., Franke, H., Loeffler, M., Wichmann, H.E., Diehl, V., 1996. Model analysis of the contrasting effects of GM-CSF and G-CSF treatment on peripheral blood neutrophils observed in three patients with childhood-onset cyclic neutropenia. *Br. J. Haematol.* 95, 616–625.
- Scholz, M., Engel, C., Loeffler, M., 2005. Modelling human granulopoiesis under poly-chemotherapy with G-CSF support. *J. Math. Biol.* 50, 397–439.
- Shankar, A., Wang, J., Rochtchina, E., Yu, M.C., Kefford, R., Mitchell, P., 2006. Association between circulating white blood cell count and cancer mortality: a population-based cohort study. *Arch. Intern. Med.* 166, 188–194.
- Shochat, E., Rom-Kedar, V., 2008. Novel strategies for granulocyte colony-stimulated factor treatment of severe prolonged neutropenia suggested by mathematical modeling. *Clin. Cancer Res.* 14, 6354–6363.
- Shochat, E., Rom-Kedar, V., Segel, L.A., 2007. G-CSF control of neutrophil dynamics in the blood. *Bull. Math. Biol.* 69, 2299–2338.
- Skeel, Roland T. (Ed.), 2007. *Handbook of Cancer Chemotherapy*, 7th edn. Lippincott Williams & Wilkins.
- Sola, Martha C., Du, Yan, Hutson, Alan D., & Christensen, Robert D. 2000. Dose-response relationship of megakaryocyte progenitors from the bone marrow of thrombocytopenic and non-thrombocytopenic neonates to recombinant thrombopoietin. *Br. J. Haematol.* 110, 449–453.
- Sparreboom, A., Wolff, A., Verweij, J., 2003. Disposition of docosahexaenoic acid-paclitaxel, a novel taxane, in blood. *Clin. Cancer Res.* 9, 151–159.
- Steinbach, K.H., Schick, P., Trepel, F., Raffler, H., Dohrmann, J., Heilgeist, G., Heltzel, W., Li, K., 1979. Estimation of kinetic parameters of neutrophilic, eosinophilic, and basophilic granulocytes in human blood. *Blut* 39, 27–38.
- Steinbach, K.H., Raffler, H., Pabst, G., Fliedner, T.M., 1980. A mathematical model of canine granulopoiesis. *J. Math. Biol.* 10 (1–12).
- Thatcher, N., Girling, D.J., Hopwood, P., Sambrook, R.J., Qian, W., Stephens, R.J., 2000. Improving survival without reducing quality of life in small-cell lung cancer patients by increasing the dose-intensity of chemotherapy with granulocyte colony-stimulating factor support: results of a British medical research council multicenter randomized trial. *J. Clin. Oncol.* 18, 395–404.
- Tjan-Heijnen, V.C.G., Wagener, D.J.T., Postmus, P.E., 2002. An analysis of chemotherapy dose and dose-intensity in small-cell lung cancer: lessons to be drawn. *Ann. Oncol.* 13, 1519–1530.
- Vainstein, V., Ginosar, Y., Shoham, M., Ranmar, D., Ianovski, A., Agur, Z., 2005a. The complex effect of granulocyte colony-stimulating factor on human granulopoiesis analyzed by a new physiologically-based mathematical model. *J. Theor. Biol.* 234, 311–327.
- Vainstein, V., Ginosar, Y., Shoham, M., Ranmar, D.O., Ianovski, A., Agur, Z., 2005b. The complex effect of granulocyte colony-stimulating factor on human granulopoiesis analyzed by a new physiologically-based mathematical model. *J. Theor. Biol.* 234, 311–327.
- Wheldon, T.E., 1975. Mathematical models of oscillatory blood cell production. *Math. Biosci.* 24, 289–305.
- Wheldon, T.E., Kirk, J., Finlay, H.M., 1974. Cyclical granulopoiesis in chronic granulocytic leukemia: a simulation study. *Blood* 43, 379–387.
- Wichmann, H.E., Loeffler, M., 1985. *Mathematical Modeling of Cell Proliferation: Stem Cell Regulation in Hemopoiesis*. CRC Press, Boca Raton.
- Zhuge, C., Lei, J., Mackey, M.C., 2012. Neutrophil dynamics in response to chemotherapy and G-CSF. *J. Theor. Biol.* 293, 111–120.